IOP Conf. Series: Materials Science and Engineering **392** (2018) 042021 doi:10.1088/1757-899X/392/4/042021

Research on wind turbines output characteristics based on complex climate and geographic conditions

Shiyou CHEN[1], Lu YIN[1], Hai LU[1] and Shi SU[1]

[1]Institute of Electric Power Reasearch,105 Yunda Western Road, Kunming, China

Abstract. Reasonable assessment of wind farm operation provides reliable wind farm operation information for dispatching, such as theoretical output, and optimization of wind farm control operation is of great significance in improving the full absorption of new energy in the regional power grid. Taking wind farms of Yunnan in the plateau mountain and three-dimensional climate conditions as objects, the theoretical output model of wind power fan is based on the precision of wind speed data. Wind farm of plateau section located in the ridge and wind resources significantly with altitude change greatly, for this situation, it is not representative and scientific to evaluate the wind speed at the wind turbine position by using wind tower, then it directly affects the accuracy of wind turbines theoretical output evaluation. For this reason, first of all, a laser radar device is used to measure the wind speed of wind turbines engine room accurately. Secondly, taking the wind speed data of lidar as reference point, the CFD simulation is used to calculate the wind speed of wind turbines in the wind farm. Finally, the calculation of wind speed and the actual output power of wind turbine which is collected from SCADA fitting, the fitting power curve is compared with the static power curve provided by the manufacturer, and the feasibility of the method is verified. The proposed strategy is applied to a wind farms in Yunnan province, the simulation results show that CFD simulation and calculation of full field wind turbine output based on the data of laser lidar wind measurement instrument, it is feasible and excellent.

1. Introduction

As a clean and convenient source of energy, wind energy is an important carrier for the development and utilization of wind power. In the past 10 years, the installed capacity of wind power in China has increased by 47 times. In 2010, the cumulative installed capacity of wind power reached 41.827 million kilowatts, ranking first in the world. It is estimated that the installed capacity of wind power in China will reach at least 150 million kilowatts by 2020, accounting for about 10%. From the above, we can see that the development prospect of wind energy is the largest. At present, the low level of energy availability of domestic wind turbines is generally 60%~70% [1], but the foreign have already reached more than 90%. So the energy efficiency of the unit still has big room for improvement even without considering the impact of power restrictions. How to reasonably evaluate the operation of wind farms and provide reliable wind farm operation information for dispatching, such as theoretical efforts, that have important significance in guiding the optimal operation and control of wind farms with the large-scale and centralized access to the main network of wind power.

With the large-scale application of wind power generation, the research on the fan output of wind farms has gradually begun. Since the theoretical power generation capacity of a wind turbine is only related to the unit parameters and the wind speed of the inflow, accurate measurement of the front wind speed of the wind turbine cabin is an important prerequisite for evaluating the theoretical output of single

and whole field units. However, in view of the fact that the high-altitude terrain wind farms are mostly distributed on ridges and the three-dimensional climate wind resources vary significantly with altitude, turbulence and wind direction are intertwined, so this traditional measurement method results in inconsistency between the wind data measured by the wind tower and the front wind speed in the wind turbine cabin. The existing literature mainly evaluates stand-alone output from wind farm output modeling and power curve rendering based on accurate wind measurement. Pan Ning[2] used the laser reflectance principle of radar anemometer to measure the wind speed and direction accurately, and used the method of interval analysis to draw the power curve of the power curve wind turbine, but the method given in the literature is only suitable for evaluating the output of a single fan that can't evaluate the fan power of the whole field. The Pan Xiong's method[3] was based on the actual wind speed of the wind farm and the historical measured data of its power generation output, established a hybrid Copula model composed of various Copula functions through the correlation processing of the wind speed series of multiple clusters within the wind farm, and then the linear superposition of the output of the multi-groups of aircrafts was used to obtain the wind farm polymerization output. The literature requires a large number of accurate wind speed historical data when performing full-field assessments. while it is difficult to obtain precise wind speeds for each aircraft group in the three-dimensional climate conditions on the plateau. The S. Gill et al. [4] used CFD numerical simulation to evaluate the wind energy distribution in the complex mountain topography which adopted a hexahedral structured grid system. The calculation converged quickly and the result was accurate. The literature provided a reliable solution for assessing the wind resources of the whole site and provided a scientific method for the assessment of the fan's output. The Kim Jaejin et al. [5] proposed a model of the real power curve, taking into account the normal distribution of wind speed data for each range. In addition, a Monte-Carlo based simulation technique was also proposed to generate wind speed data based on a formal model to provide reliable data for wind farm output modeling. The existing research has not provided a feasible experimental program for wind farm output research under the conditions of the plateau stereo climate, so it needs to be further studied. This paper proposes to use a laser radar device to measure the wind speed of wind turbines engine room accurately; then, taking the wind speed data of lidar as reference point, estimate the wind speed of wind turbines in the wind farm by CFD simulation. Finally, the estimated wind speed and the actual output power of the wind turbine are used to fit, and the fitted power curve is compared with the static power curve provided by the manufacturer to verify the feasibility of the wind field theoretical output evaluation method. The flow chart of this study is shown in Figure 1.

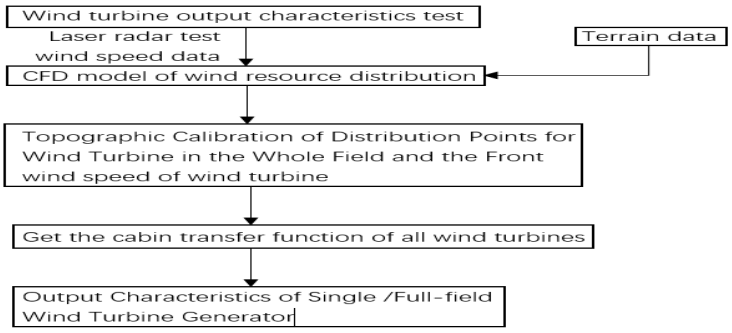

Figure1 The research flow chart

2. Single wind turbine power performance test

2.1 Laser radar wind speed measurement

Lidar is a device that uses the laser Doppler principle to track the radar echoes of particles in the air to measure the wind speed. Compared with traditional mechanical wind measurement, the laser radar can collect comprehensive wind data: wind speed, wind direction, wind shear, change, turbulence intensity, air flow inclination, etc. In addition, its measurement principle determines that the free flow wind speed

in front of the unit can be measured to ensure the reliability of the data. At the same time, it also has strong advantages in the visualization of fan wakes, atmospheric phenomena, and complex airflows [6].

2.1.1 Laser radar wind speed measurement principle

The schematic of laser radar wind speed measurement is shown in Figure 2. The optical head emits two laser beams with an angle of 2θ and uses the Doppler principle to measure the radial velocity along the laser beam. Once RWS1 and RWS0 are measured, the horizontal wind speed can be reconstructed using the following method [7].

The formula for radial wind speed is:

$$\text{RWS= Radial wind speed= Wind speed along the laser beam=}\frac{\lambda f}{2}$$

$$\lambda\text{= Laser wavelength, } f\text{= Doppler effect}$$

The two components of the horizontal wind speed can be obtained using the following formula:

$$u = \frac{RWS_0 + RWS_1}{2\cos\theta} \tag{1}$$

$$v = \frac{RWS_1 - RWS_0}{2\sin\theta} \tag{2}$$

The Wind speed vector and wind direction can be obtained by the following formula:

$$\text{HWS= Horizontal wind speed=}\sqrt{u^2 + v^2} \tag{3}$$

$$\text{wind direction=}a\tan 2(u;v) \tag{4}$$

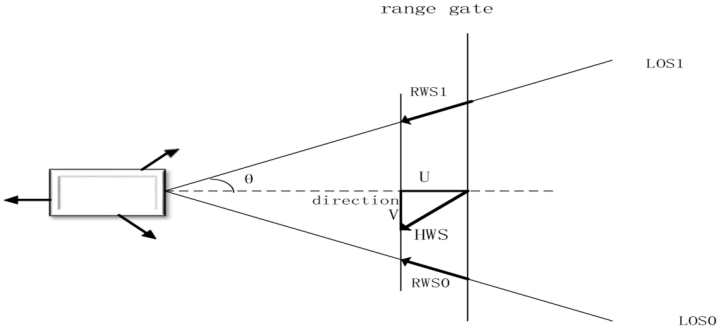

Figure2. Laser radar wind measurement

3. CFD simulation and extrapolation of the power characteristics of a single fan

CFD（Computational Fluid Dynamics） is based on the laws of fluid mechanics with the aid of a computer to solve the problem, decompose the geometric region into a small grid, and solve the complex partial differential equations in the process [8]. Combining calculation accuracy, operation time, and computer performance, using Reynolds time-average method to simulate the turbulence, Considering the surface roughness, this calculation uses WindSIM software with k-s flow model with wall function. The three-dimensional standard k-s model equation is:

$$\frac{\partial}{\partial t}(\rho k) + \frac{\partial}{\partial x_j}(\rho k u_j) = \frac{\partial}{\partial x_j}\left[\left(\mu + \frac{\mu_i}{\sigma_k}\right)\frac{\partial k}{\partial x_j}\right] + P_k - \rho\varepsilon \tag{5}$$

$$\frac{\partial}{\partial t}(\rho k)+\frac{\partial}{\partial x_j}(\rho k u_j)=\frac{\partial}{\partial x_j}\left[\left(\mu+\frac{\mu_i}{\sigma_k}\right)\frac{\partial k}{\partial x_j}\right]+ P_k-\rho\varepsilon \tag{6}$$

k and ε are turbulent kinetic energy and its dissipation rate, P_k is Turbulence energy generation terms which can be expressed by the following formula:

$$P_k=-\rho\overline{u_i^{'}u^{'}_j}\frac{\partial u_j}{\partial x_i} \tag{7}$$

In formula 6, u_j and $u_j^{'}$ are the average wind speed and fluctuating wind speed in the *j* direction. The turbulent viscosity is:

$$\mu_i=\rho C_\mu\frac{k^2}{\varepsilon} \tag{8}$$

In Equations 4, 5, and 7: $C_\mu, C_{\varepsilon 1}, C_{\varepsilon 2}, \sigma_k, \sigma_\varepsilon$ is the model constant which needs to be revised according to the wind measurement data.

3.1 Topographic data processing for complex wind farms

Topographic data is obtained by using the earth electronic terrain data ASTER GDEM (Global Digital Elevation Model for Advanced Spaceborne Thermal Emission and Reflectance Radiometers); According to the provided 1:2000 mapping topographic map (DWG format), terrain data is processed by software such as AutoCAD, Global mapper and Wasp Map Editor. The processing steps of the topographic map are as follows [9].

(1) Topographic map expansion

In addition to the wind farm area, this calculation also needs to include a surrounding area of 5000m. The topography map of the expanded area adopts ASTER electronic map data, which can truly reflect the real terrain features.

Using Autocad, Global mapper and other software to merge the original terrain data and downloaded terrain data, optimize the boundary contour and ensure the convergence of the calculation.

(2) Topographic map processing and generation

Invalid information in the terrain data is removed by CAD and only the contour information is retained;

Contour line information is processed by global mapper software, outputting the required format such as map, gws, etc.

3.2 Geomorphological data processing for complex wind farms

Rely on the global high-resolution surface coverage remote sensing mapping developed by the National Basic Geographic Information Center to obtain 30m of ground coverage data (GlobeLand30), and obtain the roughness information in the region of the wind farm by taking GLC30 roughness information and import it into the global mapper. According to the description of the geomorphological information provided in the mapping topographic map, the geomorphological information file is manually generated and imported into the global mapper file; the imported file is processed and the required format is output.

3.3 Combination and Processing of Terrain and Geomorphic Information

Topographic data is processed and combined by using the Global mapper or Wasp Map Editor, and output according to the required format of the software. The Winds needs gws file and the WT needs map file.

3.4 Calculation domain settings and discrete

CFD simulations are performed for the wind farm and its surrounding area of 5,000 meters. The parameters are set as follows:

1)Horizontal resolution

Horizontal resolution is 25m~267m. Mesh encryption is performed on the wind farm area and the wind tower area, the grid accuracy is 25m*25m, and the area outside the wind farm is gradually expanded with a coefficient of 0.3, which saves computer resources and improves the calculation speed without affecting the calculation results.

2) Number of vertical grids

The number of vertical grids is 31, and more than 10 grids below 150m are guaranteed by parameter settings to ensure the accuracy of simulation results.

3) Smooth settings

The actual terrain calculation results have good convergence, and the terrain map is not smoothed.

4) Forest model

Due to the lack of regional forest data, the forest model was not used and the roughness setting was used instead. Through the above settings, the number of grids in the x direction is 410, the number of grids in the y direction is 418, the number of grids in the z direction is 31, and the total number of grids is more than 5 million.

3.5 Boundary Condition Settings

Table 1. Wind farm boundary conditions setting parameters

Boundary and initial conditions	
Number of sectors	16
Height of boundary layer	500
Speed above boundary layer	10
Boundary condition at top	Fixed pressure
Physical models	
Potential temperature	Disregard temperture
Air density	0.91
Turbulence model	Modified
Calculation paramenters	
Solver	GCV
Convergence criteria	0.001
Number of iterations	500

4. Analysis of examples

4.1 Wind farm

The calculated wind farm is located in the Yunnan-Guizhou plateau region, where the altitude of the area is 1800-2400 m, and the altitude within the wind farm is about 500 m. The wind farm covers an area of about 30 km^2. There are a large number of mountains and ravines in the area, and the three-dimensional climate is obvious. There are a large number of medicinal plants in the area. There are 66 sets of Dongfang Electric FD82 wind turbines in the wind farm. The fan hub height is 70 m, the impeller diameter is 82 m, and the rated capacity is 1500 KW. The arrangement of the wind turbines on the site is shown in Figure 3.

The laser radar used in this experiment is the WindIris cabin laser radar produced by AVENT. In the actual test, the processing unit was placed inside the wind turbine cabin, and the optical head and the tripod hole were fixedly installed on the top of the cabin as shown in Figure 4.

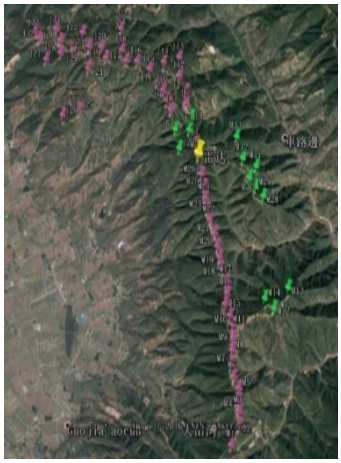

Figure3. Unit layout diagram

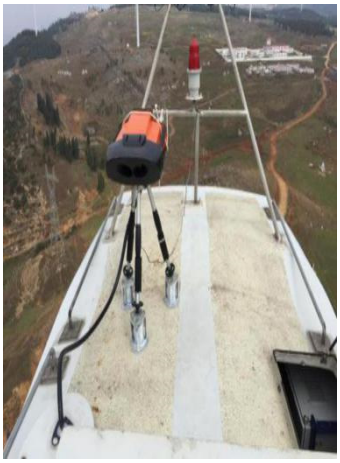

Figure4. Nacelle top installation

4.2 Calculation results and analysis

4.2.1 Validation of CFD Models and Estimation of Full Field by Radar Data

The wind speeds at 110 m, 140 m, and 170 m measured by laser radar were all imported into WindSim software to simulate the wind speed at the above position of the fan. The accuracy of the model was verified by comparing the radar velocity measurement with the prediction. The results are shown in Table 2.

Table 2. Verification of wind speed at various points

Lidar point (m)	measurement	Before calculation (m/s)	After calculation (m/s)	deviation (m/s)
	110	8.255	8.30	0.04
	140	8.253	8.3	0.08
	170	8.250	8.34	0.09
	200	8.259	8.35	0.09
	230	8.273	8.38	0.11

The 110 m measurement results and deduced results are low, and the 230 m measurement and prediction results are high. The rest of the results are in the vicinity of 8.34 m/s. The deviations are all less than 0.1. It is feasible to choose 200m(2.5D) to calculate. Because the wind wheel is blocked, the measured wind speed is smaller than the actual wind speed, and the short-distance wind speed deducing result is smaller than the long-distance. The model does not produce large errors and the result is accurate and reliable.

The CFD simulation of wind turbines in a certain region of Yunnan Province was performed, and the SCADA/anenomometer data of the turbines were collected to obtain the simulation data of each flight crew. The correlation between the deduced data and the data collected by the SCADA/anemometer was shown in Table 3. Comparing the measured SCADA data of J02~J05 and the nearby aircraft, it is found that the wind speeds of J02, J03, J04, and J05 are different from those of the surrounding aircraft. It may be caused by damage to the cabin anemometer or system error. From the table, it can be seen that the correlation between the front wind speed calculated by each fan and the SCADA/anemometer acquisition is good, and the simulation results are better [11].

Table3. Correlation between simulation results and operating results

number	SCADA Wind speed	Simulated wind speed	R^2	Wind Speed deviation	number	SCADA wind speed	Simulated wind speed	R^2	Wind speed deviation
J1	7.552	8.167	0.823	0.615	M1	7.114	6.846	0.680	-0.268
J2	6.095	7.285	0.131	1.19	M2	6.997	7.468	0.741	0.471
J3	6.096	7.311	0.112	1.215	M3	7.242	7.999	0.776	0.757

J4	6.527	7.039	0.140	0.512	M4	7.398	8.526	0.806	1.128
J5	5.264	6.685	0.123	1.421	M5	7.109	8.145	0.779	1.036
J6	7.402	7.761	0.836	0.359	M6	7.03	8.208	0.791	1.178
J7	7.442	7.556	0.726	0.114	M7	6.915	7.725	0.778	0.81
J8	6.154	7.277	0.777	1.123	M8	6.815	7.804	0.774	0.989
J9	6.077	7.148	0.767	1.071	M9	7.17	7.632	0.760	0.462
J10	6.425	7.138	0.775	0.713	M10	7.275	7.280	0.734	0.005
J11	6.206	7.423	0.749	1.217	M11	7.334	7.393	0.768	0.059
J12	6.341	6.349	0.617	0.008	M12	5.635	5.822	0.169	0.187
J13	7.534	6.915	0.671	-0.619	M13	6.874	5.979	0.248	-0.895
J14	6.53	6.747	0.702	0.217	M14	6.071	5.343	0.241	-0.728
J15	6.735	7.132	0.746	0.397	M15	7.17	7.449	0.784	0.279
J16	6.39	6.973	0.722	0.583	M16	6.645	6.669	0.759	0.024
J17	6.184	6.974	0.694	0.79	M17	6.569	6.911	0.786	0.342
J18	6.417	6.146	0.632	-0.271	M18	6.498	7.129	0.798	0.631
J19	6.202	6.654	0.653	0.452	M19	6.663	7.288	0.804	0.625
J20	5.838	6.259	0.613	0.421	M20	6.579	7.211	0.797	0.632
J21	6.091	5.554	0.546	-0.537	M21	7.006	7.629	0.818	0.623
J22	6.347	6.345	0.529	-0.002	M22	6.382	7.601	0.799	1.219
J23	6.215	6.899	0.728	0.684	M23	6.38	7.530	0.810	1.15
J24	5.454	6.805	0.706	1.351	M24	6.651	7.699	0.814	1.048
J25	4.241	5.806	0.551	1.565	M25	7.244	7.777	0.847	0.533
J26	4.457	6.612	0.599	2.155	M26	7.701	8.103	0.808	0.402
J27	5.577	6.574	0.609	0.997	M27	7.531	8.173	0.855	0.642
J28	5.686	6.413	0.590	0.727	M28	6.322	5.792	0.296	-0.53
J29	5.49	6.796	0.608	1.306	M29	5.998	6.142	0.847	0.144
J30	5.384	6.307	0.614	0.923	M30	5.598	5.762	0.850	0.164
J31	6.041	6.280	0.634	0.239	M31	6.020	6.119	0.877	0.099
J32	5.645	6.251	0.638	0.606	M32	5.338	5.583	0.883	0.245
J33	5.239	6.041	0.634	0.802	M33	5.273	5.382	0.877	0.109

4.2.2 Power curve comparison

The estimated wind speed and the actual output power of the fan are used to fit the power curve. The result of the fitting is compared with the static power curve provided by the manufacturer, as shown in Figures 5 and 6.

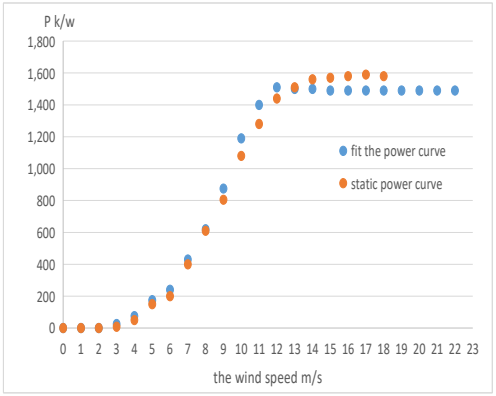

Figure5. Power curve comparison

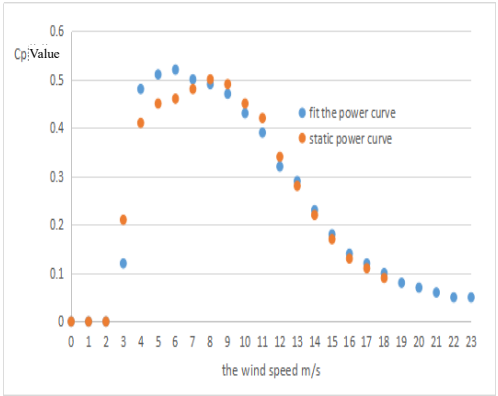

Figure6. Cp curve comparison

It can be seen from Figures 5 and 6, there are four stages in the change of power curve and Cp curve:

(1) In the low wind speed stage (3m/s~7m/s), the fitted actual power curve is slightly higher than the manufacturer's static power curve. This is mainly because static power curve simulation does not consider the effect of turbulent intensity, however, the actual power curve is affected by the turbulence intensity. At low wind speed, Cp presents an upward trend. When the wind speed increases from 3m/s

to 4m/s, the wind energy utilization coefficient Cp increases from about 0.2 to about 0.4. The increase of wind speed has a great impact on Cp. Therefore, at low wind speeds, the higher the turbulence intensity, the better the power curve performance.

(2) In the vicinity of 8m/s, the static power curve and the dynamic power curve are basically the same. Because at this stage, the variation of Cp with wind speed is very small, and the effect of turbulence intensity on wind speed cannot be reflected in the power curve.

(3) In the vicinity of the rated power (9m/s~12m/s), the fitted actual power curve is lower than the static power curve of the manufacturer. This is because the Cp curve begins to decline, which is the opposite of the low wind speed segment, and thus has the above performance.

(4) When exceeding the rated wind speed (13m/s~25m/s), the actual output power of the fan is higher than the rated power. This is because the fan can be designed to generate about 10% more energy, which is higher than the static power curve.

In summary, the power curve fitted by laser radar wind measurement and CFD extrapolation fan output method is more in line with reality. And this method is feasible.

5. Conclusion

In this paper, firstly, under the complex terrain and climate conditions, traditional wind measurement methods cannot accurately measure the front wind speed of the nacelle, and laser radar is used to accurately measure the wind speed at different distances in front of a single nacelle in an area in Qujing, Yunnan, and correlation analysis of wind measurement data is performed. This demonstrates the reliability of laser radar wind measurement data; Then, the wind speeds measured by Lidar at 110m, 140m, and 170m were all imported into WindSim software. The wind speed of the whole site was simulated. The simulation results were compared with the wind speed measured at the wind tower, and it was concluded that the CFD simulation scheme was feasible; Finally, the CFD simulation of the calculated wind speed and the actual output power of the wind turbine was used to fit the power curve, and the result of the fitting was compared with the static power curve provided by the manufacturer. The result shows that the curve obtained by fitting is consistent with the static power curve provided by the manufacturer. The feasibility of using CFD simulation to extrapolate full-field theoretical power scheme based on lidar wind measurement is verified.

References

[1] Ma Ping, Liu Changhua Wind turbine power curve verification（ Renewable Energy Resources） p 26（12）：82-84.

[2] Pan Ning Research on Test Method of Wind Turbine Power Curve Based on Lidar Wind Instrument (Energy Conservation Technology) p 31（178）：112-115.

[3] Pan Xiong, Wang Lili, et al. Modeling method of wind farm output based on mixed Copula function (Automation of Electric Power Systems) p 38(14): 17-22.

[4] S. Gill, B. Stephen, S. Galloway Wind turbine condition assessment through power curve copula modeling（IEEE Transactions on Sustainable Energy） p 3(1) :94-101

[5] Kim Jaejin,Baik Jongjin A numerical study of the effects of ambient wind direction on flow and dispersion in urban street canyons using the RNG k-s turbulence model (Atmospheric Environment) p 38(19)：3039-3048.

[6] Xiao Chuangying， Wang Ningbo， Dou Jing， et al. Analysis on Wind Power Output Characteristics of Jiuquan in Gansu Province (Automation of Electric Power Systems) p 34（17）：64- 67.

[7] Liu Hao, Liu Yibing, Xin Weidong, Li Ruozhao Analysis of Power Characteristics of Wind Turbine Based on Operational Data (Power System and Clean Energy) pp53-56.

[8] P. Mohan Kumar ,M. Mohan Ram Surya, et al. Comparitive CFD analysis of darrieus wind turbine with NTU-20-V and NACA0018 airfoils (Singapore: 2017 IEEE International Conference on Smart Grid and Smart Cities).

[9] Xiao Yiqing，Li Chao，et al. CFD method for evaluating wind energy in complex terrain (Journal of South China University of Technology) pp 30-35.
[10] Bian Haihong，Zheng Weigao，Lin Zhangsui，et al. Modeling and Application of Statistical Indicators for Cluster Wind Farm Output (Electric Power Automation Equipment) pp 21-27.
[11] Bian Haihong, Zheng Weigao, Lin Zhanghui, et al. Modeling and application of statistical index of cluster wind farm output (Electric Power Automation Equipment) pp 12-27.